Journal of Ceramic Processing Research. Vol. 24, No. 6, pp. 1042~1049 (2023)
(Received 24 May 2023, Received in revised form 12 December 2023, Accepted 12 December 2023)
https://doi.org/10.36410/jcpr.2023.24.6.1042

J O U R N A L O F
Ceramic Processing Research

Mixed alkali effect on the thermal properties of SiO_2-B_2O_3-ZnO-K_2O-Na_2O glass system

Sungmin Son and Seunggu Kang*
Department of Advanced Material Engineering, Kyonggi University, Suwon, Kyonggi-do 16227, South Korea

In this study, we explored the thermal and mechanical properties of a SiO_2-B_2O_3-ZnO-K_2O-Na_2O (SBZKN) glass composition for potential use in vacuum insulated glass windows. The glass's physical properties were controlled through the mixed alkali effect, with K_2O and Na_2O serving as network modifiers, maintaining a fixed total of 20%. The SBZKN composition powder vitrified below 1000 °C. Varying the K_2O content from 0% to 20% resulted in reduced density and hardness of the glass specimen. DTA analysis indicated decreasing glass transition temperature (Tg) and crystallization temperature (Tp) with higher K_2O content, reaching a minimum at 10%. The coefficient of thermal expansion peaked at 10% K_2O content, and thermal conductivity was lowest with 15% K_2O content. Heating a cube-shaped glass specimen (700 to 800 °C) caused semicircular spreading due to glass viscosity. Contact angle between spread glass and substrate decreased with temperature but generally increased with K_2O content. At 800 °C, all specimens showed excellent wetting with contact angles of 44° to 72°. This study provides evidence of alkali mixing effects on thermal and mechanical properties, contributing vital data for future vacuum insulated glass window design and development.

Keywords: Vacuum-insulated-glass, Spacer, SBZKN-glass, Mixed-alkali-effect.

Introduction

Energy efficiency and environmental friendliness are key considerations in modern architecture and construction. Research efforts have focused on developing technologies that minimize heat transfer through building envelopes to reduce energy loss [1-3]. Glass, as a representative ceramic material, is widely utilized in building envelopes due to its exceptional properties such as abrasion resistance, thermal stability, corrosion resistance, and transparency [4-6].

However, conventional glass windows exhibit relatively low thermal insulation performance compared to the building walls, and it is estimated that approximately 45% of total heat loss in a building occurs through windows [7]. To meet the growing demand for larger and more numerous windows in architectural design, it is crucial to enhance the thermal insulation performance of glass windows. Various technologies have been developed for this purpose, including low-emissivity coatings, double-glazed windows, triple-glazed windows, and gas injection windows, which improve insulation capabilities [8-10]. The first method employed in enhancing the thermal insulation of windows is by applying a low-emissivity (low-e) coating to the glass surface. This coating serves the purpose of reflecting infrared radiation and preventing the absorption or emission of heat from both the building's interior and exterior. It is commonly referred to as low-e coating windows and is instrumental in maintaining thermal insulation within the building. The second method involves the incorporation of a gap between two glass panes, which is either filled with a low-conductivity gas or kept as a vacuum. When the gap is filled with air, it is known as double-glazed windows. Alternatively, if the gap is filled with gas, it is referred to as gas-injection glass. Lastly, when a vacuum is established within the gap, it is termed vacuum-insulated glass (VIG). Additionally, a combination of these methods entails placing a low-e coated film between the two glass panes, resulting in what is known as triple-glazed windows.

Among these techniques, vacuum-insulated glass (VIG) has recently garnered significant attention [11]. The spacer plays a crucial role in supporting and stabilizing the gap between the two glass panes in the VIG system. The spacer is responsible for maintaining a consistent distance between the glass panes, thereby preserving the vacuum seal and preventing any undesirable movement or distortion. By effectively supporting the gap, the spacer ensures the long-term functionality and structural integrity of the VIG system, contributing to its overall performance in terms of thermal insulation and energy efficiency

The concept of vacuum insulated glass (VIG) windows gained practical significance with Robinson et al.'s

*Corresponding author:
Tel : +82-31-249-9767
Fax: +82-31-249-9774
E-mail: sgkang@kyonggi.ac.kr

publication on its insulation properties in 1989 [12]. This was followed by the commercial availability of the first VIG product by Nippon Sheet Glass group in 1996, which prompted further ongoing research [13]. The thermal performance of VIG is strongly influenced by factors such as the frame, glass edges, and spacer supporting the glass substrate [7]. In a VIG system, spacers play a critical role in preserving the gap between the glass panes and providing structural support. To achieve effective thermal insulation in a vacuum insulated glass (VIG) system, it is essential to maintain a low internal pressure, typically below 10^{-3} torr. However, this creates a pressure differential between the external atmospheric pressure and the internal pressure, resulting in bending stress on each glass pane. Such stress can cause distortion and lead to glass breakage, compromising the insulation effectiveness of the system. Therefore, the use of spacers becomes crucial in addressing these challenges from an engineering standpoint [11]. In addition, considering the fabrication process temperature range of 700-800 °C, the wetting characteristics and compatibility of thermal expansion coefficients between the glass plates and spacer become vital factors.

Traditionally, glass and metal have been used as spacer materials; however, these materials present several challenges and limitations. Firstly, metals have relatively high thermal conductivity, which leads to easy heat transfer. This drawback increases heat loss and diminishes the efficiency of heating and cooling systems. Secondly, metals exhibit irreversible thermal expansion characteristics, causing deformations in the spacer distance and overall structure with temperature fluctuations. These factors can adversely impact the long-term reliability and performance of the system [14-16].

In this study, the choice of glass as the spacer material was made to address these limitations from an engineering perspective. Glass offers a lower thermal conductivity, making it difficult for heat to transfer, thus enhancing thermal insulation. Furthermore, glass exhibits less irreversible thermal expansion compared to metals, resulting in minimal deformations and ensuring long-term stability [17-19]. Additionally, glass possesses high optical transparency, improving visibility through the glass and promoting natural lighting. Consequently, considering these advantages, glass was selected as the spacer material in this study.

The mixed alkali effect, involving nonlinear changes when different alkali metal ions, such as sodium (Na) and potassium (K), are combined in glass composition, influences the thermal and structural properties of multi-alkali glass systems [20, 21]. First identified by Weber in 1883 during Thermometer Effect studies, this phenomenon results from interactions between distinct alkalis [20, 22-24]. At specific ratios, the mixed alkali effect exhibits minimum or maximum properties, underscoring its significance [25]. Despite numerous proposed models, the exact scope and structural relationship of this phenomenon remain unclear [23, 26-29]. The 'substructure model' stands out among these models, wherein substituted alkali metal ions form subnetworks within the glass structure. Each subnetwork, characterized by different properties like ion size and oxygen ion interactions, competes and interacts, influencing the glass structure and physical properties, ultimately altering the coefficient of thermal expansion.

Commercial glass compositions often integrate mixed alkalis to enhance properties compared to single alkali compositions. Various studies, including those by Dilmore [30]. Zhifang [31] and others, have explored the mixed alkali effect's influence on the durability of Na_2O-K_2O-CaO-SiO_2 glasses. Simultaneously, X. Wang [32] examined the substitution effect of Na_2O and K_2O in the Na_2O-K_2O-CaO-P_2O_5-SiO_2 glass system, and Y. Onodera [33] investigated positional changes of alkali ions around non-bridging oxygen atoms induced by the mixed alkali effect in the SiO_2-Na_2O-K_2O glass system.

In this study, a high-functionality spacer for VIG was developed using SiO_2-B_2O_3-ZnO-K_2O-Na_2O (SBZKN) glass. B_2O_3 and ZnO were added to facilitate low-temperature processing. The modifier content was fixed at 20%, but the replacement of Na_2O with K_2O led to a mixed alkali effect. The mechanical properties of the glass, including density and hardness, were analyzed. Compatibility with plate glass and co-fired processability were assessed through measurements of thermal expansion coefficient and high-temperature contact angle. Finally, the suitability of the glass as a spacer in vacuum insulated glass was evaluated.

Experimental

The raw materials used in this study were SiO_2 (Kojundo Chemicals, Ltd., 99.9%), B_2O_3 (Kojundo Chemicals, Ltd., 99.9%), ZnO (Kojundo Chemicals, Ltd., 99.9%), K_2CO_3 (Kojundo Chemicals, Ltd., 99.9%) and Na_2CO_3 (Kojundo Chemicals, Ltd., 99.9%). The composition of SiO_2-B_2O_3-ZnO-K_2O-Na_2O (SBZKN) glass is shown in Table 1. The mixture was prepared according to the specified ratios and milled using a zirconia ball mill for 12 hours. The prepared materials were then placed in an alumina crucible and melted at 1000 °C for 2 hours using an SiC electric furnace. The molten glass was poured into preheated graphite molds at 300 °C and rapidly quenched. Subsequently, annealing was carried out for 2 hours to minimize residual internal stresses in the glass and prevent breakage followed by natural-cooling to room temperature.

The crystallographic analysis of the prepared glass was performed using X-ray diffraction (XRD) with Cu-Kα (1.5406 Å) radiation, utilizing a MiniFlex II instrument (Rigaku Co., Japan) in the range of 5° to 90° (30 kV, 15 mA, scan speed of 4°/min, 2θ step of

Table 1. Composition of SBZKN glass system fabricated in this study (mol%).

Specimen	SiO_2	B_2O_3	ZnO	K_2O	Na_2O
0 K				-	20
5 K				5	15
10 K	40	20	20	10	10
15 K				15	5
20 K				20	-

0.02°). The density of the glass was measured using the Archimedes principle (KS L ISO18754). For thermal characterization of each composition, the glass was ground to particle sizes below 45 μm and subjected to differential thermal analysis (DTA) using an SDT650 instrument (TA Instruments, USA) with a heating rate of 10 °C/min. The surface hardness of the glass was measured using a Nanoindenter (NanoTest Vantage Platform, Micro Materials Ltd., UK) under a load of 100 mN.

The coefficient of thermal expansion was measured using a Thermomechanical Analyzer (TMA Q400, TA Instruments, USA) at a heating rate of 10 °C/min in the temperature range of room temperature to 500 °C. Thermal conductivity was measured using a Laser Flash Apparatus (LFA457 MicroflashTM, Netzsch, Germany). A high-temperature microscope (DM2500, Leica, Germany; TS1500 heating stage, Linkam Scientific Inst., UK) was used to observe behavior change during heating for cube-shaped glass, and the contact angle changes were measured using the "Image J" program.

Results and Discussion

The XRD analysis results of the glass fabricated in this study are shown in Fig. 1, exhibiting typical broad peaks characteristic of amorphous materials.

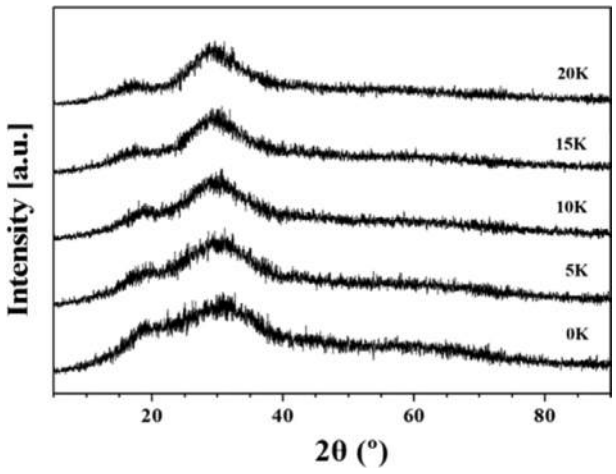

Fig. 1. XRD pattern of SBZKN glass system according to amount of K_2O substituted for Na_2O.

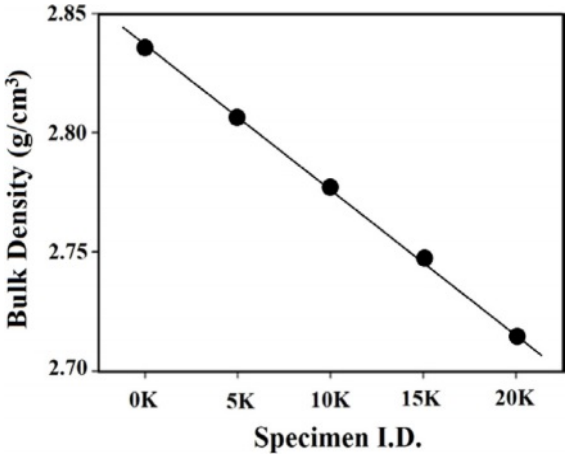

Fig. 2. Density of SBZKN glass system according to amount of K_2O substituted for Na_2O.

However, it was observed that the full width at half maximum (FWHM) of the broad peak, representing the amorphous nature, slightly decreased with an increase in K_2O content.

The measured bulk density is shown in Fig. 2. Density decreased linearly with increasing K_2O content. This is the result of the expansion of the glass network structure as Na^+ ions with a radius of 102 pm are replaced with larger-sized K^+ ions with a radius of 138 pm.

The addition of larger K^+ ions compared to Na^+ ions is believed to alter the electrostatic cationic field on the anion as shown in Eq. (1) and (2), affecting the density. The Coulombic force [34] between the two ions, F_c, is given by:

$$F_C = \frac{(Z_c e)(Z_a e)}{a^2} \quad (1)$$

where, $a = r_c + r_a$ (r_c and r_a mean radius of cation and anion, respectively)

e = electronic charge (4.8×10^{-10} esu)

Z_c and Z_c = valence of the cation and anion, respectively

Since the Z value of oxygen ions in oxide glass and electronic charge are constant, Eq. (1) simplifies to Eq. (2) [34] for comparing Fc between oxide glasses,

$$F_C = \frac{Z_c}{a^2} \quad (2)$$

Eq. (2) represents the force between ions, the Coulomb force, as the electrostatic cationic field on the anion from the perspective of a cation ion. According to Eq. (2), as the radius of the added ion decreases, the electrostatic cationic field on the anion of the added K^+ ion decreases. This results in a weaker attraction force on the surrounding non-bridging oxygens and ultimately weakens the contraction force on the glass network structure [30-33, 35-37].

Fig. 3 illustrates the DTA results for glasses with varying amounts of K_2O substituting Na_2O. (a) Displays

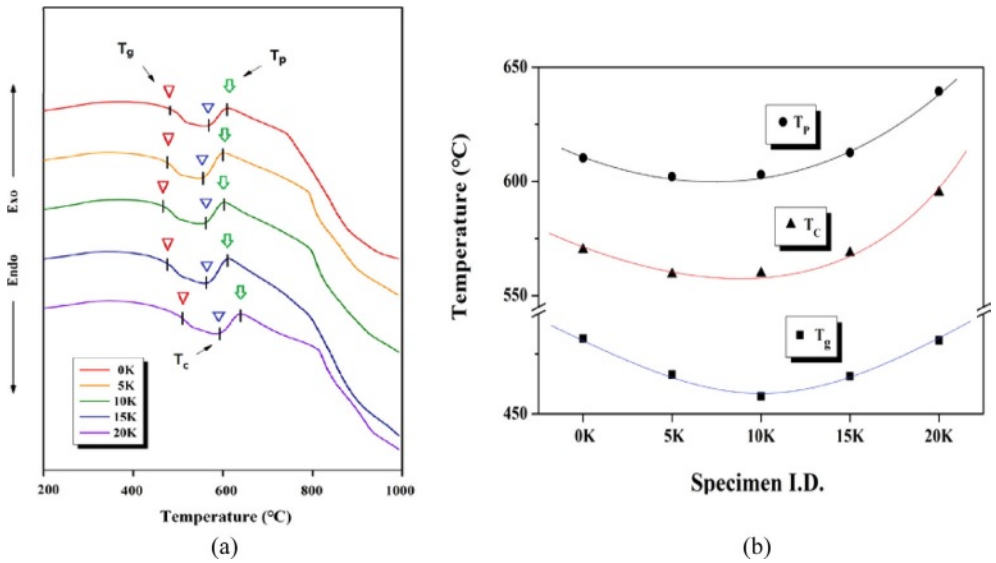

Fig. 3. (a) DTA curves of SBZKN glass system according to amount of K_2O substituted for Na_2O, and (b) specific temperatures obtaind from DTA curves shown in (a).

the DTA curves of the SBZKN glass system, while (b) shows specific temperatures derived from the DTA curves in (a). The glass transition temperature (T_g), crystallization initiation temperature (T_c), and temperature of maximum crystallization rate (T_p) are represented.

T_g decreases from 481 °C to 457 °C in samples with a 10 K increase in K_2O substitution, followed by an increase to 481 °C in 20 K samples. This phenomenon resembles the isokom temperature changes of T_g in glass with substitution of Na_2O and K_2O alkali oxides, which depend on the Na_2O/K_2O [32, 38-39]. Both T_c and T_p exhibit a minimum value at 10 K as the K_2O content increases, clearly demonstrating the mixed alkali effect on both the glass transition temperature and specific crystallization-related temperatures.

Fig. 4 illustrates the variations in hardness of the samples measured by nano-indentation as a function of K_2O content. The graph displays the displacement of the indenter in the depth direction in relation to the applied load. The left side of the loop represents the displacement during loading, while the right side represents the displacement during unloading as shown as arrows in Fig. 4.

During the indentation process, a combination of elastic and plastic deformations occurs, resulting in complex deformation at the specimen surface. This leads to different displacement directions during loading and unloading, as depicted in the graph. The hardness value, denoted as H, is calculated using Eq. (3):

$$H = P_{max} / A \quad (3)$$

Here, P_{max} represents the maximum applied load on the sample, and A is the area of the residual impression

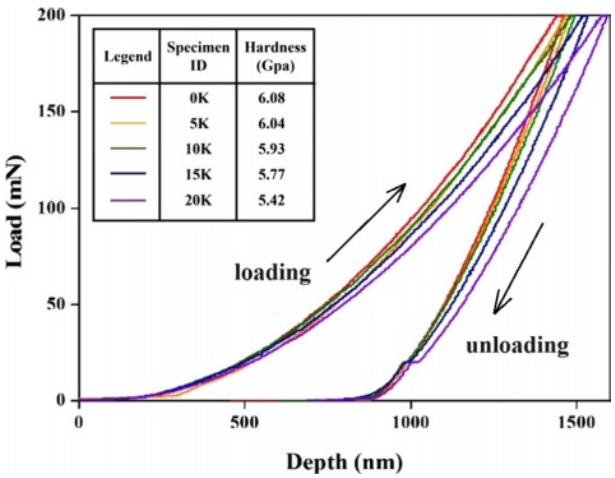

Fig. 4. Micro hardness curves of SBZKN glass system according to amount of K_2O substituted for Na_2O.

left on the sample after the indenter is unloaded.

Higher K_2O substitution in the samples increases displacement during loading, attributed to expanded glass network structure and increased molar volume from larger K^+ ions. Hardness decreases with rising K_2O content, with the 20 K sample showing an 11% reduction compared to the 0 K sample. Substituting Na_2O with K_2O leads to increased molar volume and decreased density, as the larger K ions open up the glass network structure. As shown in Fig. 2, as K_2O substitution increases, molar volume rises, resulting in lower density and reduced resistance to external forces. Fig. 4 indicates that the depth of indentation by a nano-indenter increases with more K_2O, leading to decreased hardness due to the larger K ion radius. The experimental results in this study align with prior research findings.

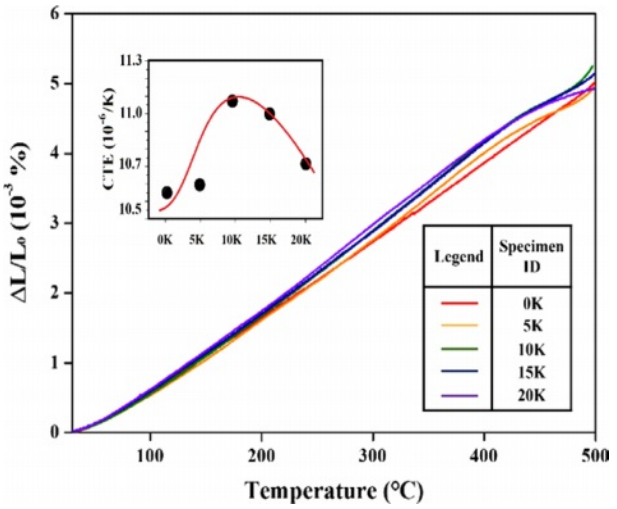

Fig. 5. Change in length per unit length with temperature of SBZKN glass system as a function of amount of K_2O substituted for Na_2O. Linear coefficients of thermal expansion (CTE) are inserted in small square in the upper left of the figure.

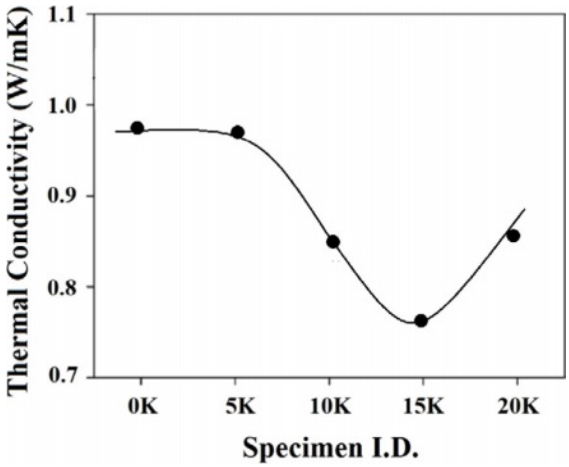

Fig. 6. Thermal conductivity of SBZKN glass system according to amount of K_2O substituted for Na_2O, measured at RT ~ 500 °C.

El-Moneim et al. [40] reported reduced microhardness when substituting Na_2O with K_2O in silicate glass, ranging from 0 to 15 mol%. Similarly, Greene et al. [41] confirmed that higher K_2O content in silicate-based multi-component glasses resulted in decreased density and microhardness.

Fig. 5 depicts the change in length per unit length of the SBZKN glass system with temperature as a function of the amount of K_2O substituted for Na_2O. The linear coefficients of thermal expansion, calculated from the graphs of change in length per unit length vs. temperature, are displayed in a small square in the upper left corner of the figure.

The linear coefficient of thermal expansion (CTE) is an engineering metric that represents the relationship between length change and temperature change. This coefficient can be calculated using a graph by first identifying the linear region and selecting two points within that region. By measuring the length change and determining the temperature difference between the chosen points, the coefficient can be calculated using the following formula:

$$CTE = \frac{length\ change}{(initial\ length)(temperature\ change)} \quad (4)$$

The thermal expansion coefficient demonstrates a trend of increasing and then decreasing as the amount of K_2O substitution increases. This observation aligns with the commonly known principle that glasses with lower T_g values tend to have higher thermal expansion coefficients [39, 42-43].

When the cationic species in glass are replaced by cations with larger radii, the field strength of the cations weakens, as shown in Eqs. (1) and (2). The field strength, in the context of glass composition, refers to the electric field strength associated with cations. This weakening influences the bonding between the substituted cations and oxygen ions, resulting in weaker overall structural integrity. Therefore, when glass is subjected to heat, the thermal vibration amplitude around non-bridging oxygen (NBO) increases, leading to a higher coefficient of thermal expansion for the glass. These findings are consistent with the research results of Greene [41] and Shah [44]. Greene et al. [41] found that with an increase in the mol ratio of K_2O in silicate-based multi-component glasses, the density decreased while the thermal expansion coefficient increased. Similarly, Shah et al. [44] confirmed that in phosphate glasses, an increase in the mol% of K_2O within the range of 15 to 33 mol% led to an increase in the thermal expansion coefficient.

Fig. 6 illustrates the thermal conductivity as a function of K_2O content within the RT~500 °C range. The thermal conductivity of the glass samples decreases with increasing K_2O substitution, reaching a minimum value at the 15 K sample. Higher density generally improves thermal conductivity as it provides more atoms for heat transfer. Fig. 2 shows that substituting Na_2O with K_2O decreases density due to the larger ionic radius of K ions, opening the glass structure. Consequently, thermal conductivity, proportional to density, decreases with K_2O substitution up to 15% (see Fig. 6). Beyond 15%, thermal conductivity increases, possibly due to the mixed alkali effect. In glass formulations with single oxides (Na_2O or K_2O), conductivity is high. However, mixing these oxides creates substructures with a competitive relationship, leading to increased phonon scattering. Up to 15%, the structural opening effect of K ions controls thermal conductivity; beyond 15%, decreased phonon scattering due to substructure competition increases it. Accuracy in interpretation requires further experimentation and analysis

In the interpretation of the presented data, the

mentioned mixed alkali effect is a phenomenon commonly observed in alkali silicate glass. This occurs when two different alkali metal ions, such as sodium (Na) and potassium (K), are combined in the glass composition, influencing the thermal and structural properties. Specific ratios reveal minimum or maximum properties, underscoring the significance of the mixed alkali effect [25]. One explanation for the 'mixed alkali effect' is the 'subnetwork model.' This model arises when substituted alkali metal ions form subnetworks within the glass structure, each with distinct characteristics like ion size and interactions with oxygen ions. These subnetworks compete and interact, playing a decisive role in modifying the glass structure and its various physical properties.

Beyond density and the mixed alkali effect, various factors, including the atomic structure's vibrational modes, can impact thermal conductivity. Phonons, similar to sound waves, play a role in carrying thermal energy through the glass, with their interaction affecting overall thermal conductivity. Glass's thermal conductivity is further influenced by its composition, network structure, temperature, and porosity [45-47]. However, it's crucial to clarify that in interpreting the current experimental data, my analysis focused primarily on density and the mixed alkali effect. Therefore, for a more detailed and accurate analysis, additional experiments are needed. We want to emphasize that while we briefly touched upon various factors, the current interpretation is based on the limited scope of this study. We acknowledge the importance of further experiments to enhance the depth of our analysis

In order to investigate the high-temperature viscosity behavior according to the K_2O substitution level, the measured contact angles at different temperatures and the pictures taken with a high-temperature microscope of the shape of the specimen produced by viscous flow at high temperature are presented in Fig. 7 and 8, respectively. The contact angle is one of the important factors that determines the wetting characteristics between the glass plate and glass spacer in a vacuum-sealed glass.

Generally, better wetting characteristics are achieved when the contact angle is smaller. When the angle exceeds 90°, the glass does not spread on the substrate due to surface tension, and since the sphere shape is maintained almost as it is, it is difficult to bond with the substrate. In this experiment, the contact angle between the substrate and glass decreased with increasing temperature, and it also showed an increasing trend with an increasing K_2O substitution level. However, in the range of 700-750 °C, there was a slight decrease in the contact angle for the 5 K sample compared to the 0 K sample. An accurate analysis of the temporary decrease in contact angle at low temperatures requires additional research. At 800 °C, all samples showed excellent wetting characteristics with contact angles ranging from 44° to 72°. However, when heated to

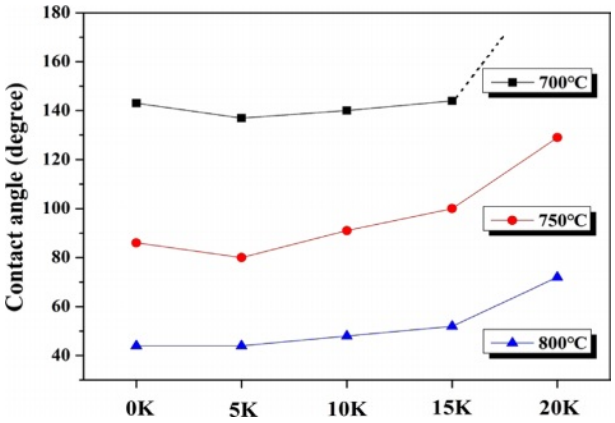

Fig. 7. Contact angle of SBZKN glasses according to amount of K_2O substituted for Na_2O at various temperatures.

750 °C, samples with K_2O content of 5-10% exhibited contact angles in the range of 80° to 90°, and the contact angles of all samples exceeded 130° at 700 °C, In particular, a significant increase in the contact angle was observed when the composition changed from 15 K to 20 K at all temperatures.

Fig. 7 and Fig. 8 present the measured contact angles at different temperatures and images captured using a high-temperature microscope to observe the shape of the specimen produced by viscous flow at high temperature, respectively. These investigations aim to examine the high-temperature viscosity behavior concerning the level of K_2O substitution. The contact angle plays a crucial role in determining the wetting characteristics between the glass plate and glass spacer in a vacuum insulated glass system. Generally, better wetting characteristics are achieved when the contact angle is smaller. If the angle exceeds 90°, the glass does not spread on the substrate due to surface tension, making it difficult to bond effectively.

In this experiment, the contact angle between the substrate and glass decreased with increasing temperature, while it exhibited an increasing trend with higher levels of K_2O substitution. However, in the temperature range of 700-750 °C, a slight decrease in the contact angle was observed for the 5 K sample compared to the 0 K sample. A more accurate analysis of this temporary decrease in contact angle at lower temperatures requires further research. At 800 °C, all samples demonstrated excellent wetting characteristics with contact angles ranging from 44° to 72°. However, when heated to 750 °C, samples with K_2O content of 5-10% exhibited contact angles in the range of 80° to 90°, and the contact angles of all samples exceeded 130° at 700 °C. Notably, a significant increase in the contact angle was observed when transitioning from the 15 K to 20 K composition at all temperatures.

Considering that the typical process temperature for vacuum insulated glass windows falls within the range of 700-800 °C, the samples exhibiting excellent wetting

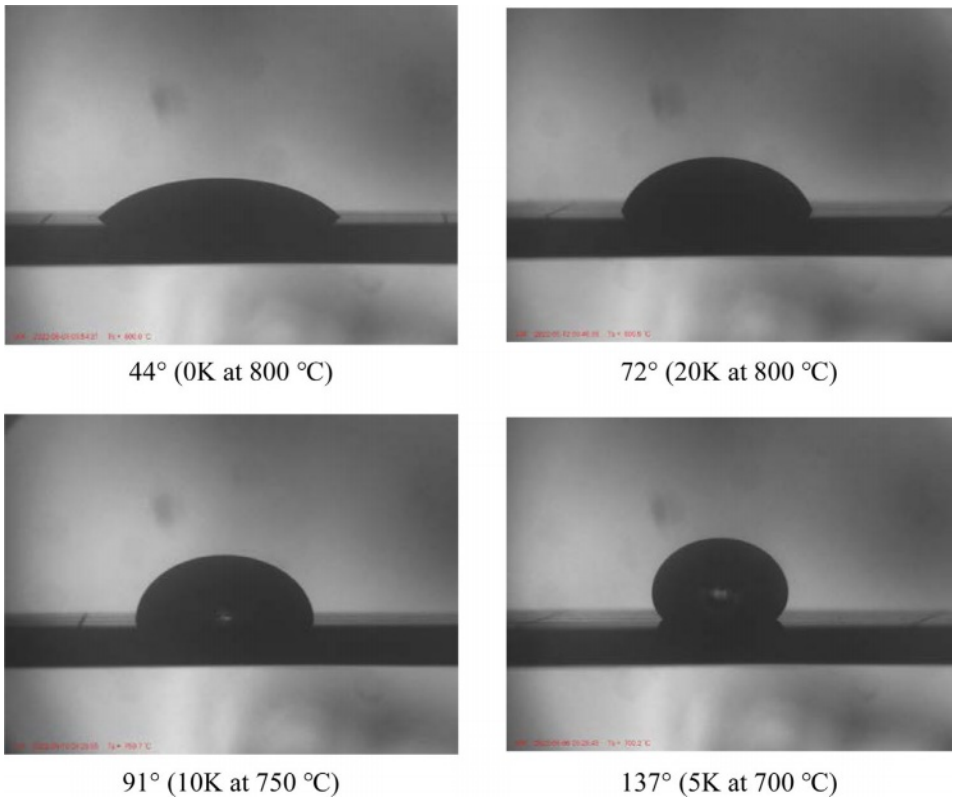

Fig. 8. Photos showing the wetting behavior with contact angle between the SBZKN glass specimen and the substrate taken with a high-temperature microscope.

at 800 °C are the 0-15 K samples. When the process temperature is lowered to 750 °C, it is deemed that the 0-10 K specimens possess usable wetting characteristics. However, when the process temperature is set to 700 °C with this particular glass system, there is a concern regarding spacer separation during usage due to weak adhesive strength between the spacer and the glass plate.

In summary, the study revealed the presence of a mixed alkali effect in various properties of the glass, including glass transition temperature, crystallization temperature, thermal expansion, thermal conductivity, high-temperature contact angle, density, and hardness. Furthermore, it was observed that these properties can be controlled by substituting K_2O. Thus, by adjusting the ratio between modifiers while keeping the glass composition relatively consistent, it becomes possible to manipulate the properties of the glass. This presents a viable method for selecting spacer materials in vacuum insulated glass windows that can meet the desired specifications of designers and consumers. The observed mixed alkali effect in this study serves as evidence of this feasibility.

Conclusions

In this study, the SBZKN glass composition was specifically designed to produce a low-melting glass that can be melted at 1000 °C. The K_2O/Na_2O ratio in the modifier was adjusted to control the mechanical and thermal properties of the glass. Based on the findings, the following conclusions were drawn:

The composite alkali effect resulted in the minimum values of glass transition temperature (T_g) and maximum crystallization temperature (T_p) around the K_2O/Na_2O=1 composition. The coefficient of thermal expansion increased with an increase in K_2O substitution, reaching a maximum value for samples with K10 to K15 compositions. The coefficient of thermal expansion increased with the K_2O content, peaking at 10% K_2O content. Thermal conductivity was lowest in specimens with 15% K_2O content. Increasing the K_2O substitution led to an increase in high-temperature viscosity, thereby increasing the contact angle between the substrate and glass, while the contact angle decreased with increasing temperature. Compared to the glass with single alkali composition, the mixed alkali effect was observed in the glass temperature and crystallization temperature, thermal expansion coefficient, thermal conductivity, and wetting angle of the glass with complex alkali composition. However, the mechanical properties, such as molar volume and hardness, exhibited a rule of mixture effect rather than the mixed alkali effect. Substituting K_2O for Na_2O in the SBZKN glass composition resulted in an expansion of the glass network structure, leading to a decrease in bulk density and hardness.

In summary, the study demonstrates the advantages

of the SBZKN glass composition in terms of its low-melting temperature, mixed alkali effect, and the ability to control desired properties for vacuum insulating glass windows. These findings offer promising prospects for practical implementation and meeting the needs of designers in this field.

Acknowledgements

This work was supported by Kyonggi University Research Grant 2020. We thank to Mr. Suh from Fulan Korea Co. for his valuable discussions.

References

1. M. Harikarana, P. Kulanthaivelb, A.R. Krishnarajac, and P.C. Murugand, J. Ceram. Process. Res. 24[2] (2023) 266-273.
2. S. Shanmughana, S.K. Kaliyannanb, S. Marasamyc, and P. Thiyagarajand, J. Ceram. Process. Res. 24[1] (2023) 111-119.
3. S. Janania, G.S. Rampradheepb, P. Kulanthaivelc, and P.C. Murugand. J. Ceram. Process. Res. 23[6] (2022) 884-891.
4. D. Hülsenberg, A. Harnisch, and A. Bismarck, in "Microstructuring of Glasses" (Springer Berlin Heidelberg, 2008) p. 57-69.
5. W. Höland and G.H. Beall, in "Glass-Ceramic Technology" (John Wiley & Sons, Inc., 2012) p. 38-74.
6. T.W. Ha and S.G. Kang, J. Ceram. Process. Res. 23[2] (2022) 237-242.
7. C.H. Jeong, M.S. Yeo, and K.W. Kim, J. Asian Archit. Build. Eng. 14[3] (2015) 717-724.
8. R. Tafakkori and A. Fattahi, Sustain. Energy Technol. Assess. 43 (2021) 100919.
9. S. Memon, in "Design, fabrication and performance analysis of vacuum glazing units fabricated with low and high temperature hermetic glass edge sealing materials" (PhD thesis, Loughborough University, 2013) p. 6-34.
10. I. Pérez-Grande, J. Meseguer, and G. Alonso, Appl. Therm. Eng. 25[17-18] (2005) 3163-3175.
11. B.P. Jelle, S.E. Kalnæs, and T. Gao, Energy Build. 96 (2015) 329-356.
12. S.J. Robinson and R.E. Collins, in Proceedings of the ISES World Congress, September 1989, edited by L. Broman and G. Eriksson (Int. Solar Energy Soc. 1989) p. 1.
13. A. Zoller, in "Hohle Glasscheibe" (Deutsches Reich Patents Nr. 387655, 1913) p. 1.
14. H. Riedel, S. Mokdad, I. Schulz, C. Kocer, P.L. Rosendahl, J. Schneider, M.A. Kraus, and M. Drass, Automation in Constr. 135 (2022) p. 104144.
15. K. Swimm, H. Weinläder, and H-P. Ebert, Int. J. Thermophys 30 (2009) p. 934-948.
16. F. Zoller, in "Hollow pane of glass" (German Patent 387655, 1924) p. 1.
17. O. Kaygili, F. Yakuphanoglu, and C. Tatar, J. Ceram. Process. Res. 17[8] (2016) 881-884.
18. F. Heydari, A. Maghsoudipoura, M.O. Shabania, Z. Hamnabardb, and S. Farhangdousta, J. Ceram. Process. Res. 15[1] (2014) 35-43.
19. R. Souaga, N. Kamelb, D. Moudirb, Y. Mouhebb, and F. Aouchicheb, J. Ceram. Process. Res. 23[3] (2022) 304-311.
20. H.J. Jeong, D.W. Jeon, J.H. Kim, Y. Lee, M. Lee, J. Hwang, H. Park, H. Lim, J. Lee, T. Park, and D. Shin, J. Ceram. Process. Res. 17[7] (2016) 694-698.
21. O.P. Thakur, D. Kumara, O. Parkasha, and L. Pandeyb, J. Ceram. Process. Res. 5[2] (2004) 106-113.
22. J.O. Isard, J. Non-Cryst. Solids. 1[3] (1969) 235-261.
23. C.J. Wilkinson, A.R. Potter, R.S. Welch, C. Bragatto, Q. Zheng, M. Bauchy, M. Affatigato, S.A. Feller, and J.C. Mauro, J. Phys. Chem. B. 123[34] (2019) 7482-7489.
24. D.E. Day, J. Non-Cryst. Solids. 21[3] (1976) 343-372.
25. X. Ma, Y. Xu, J. Cheng, S. Sun, Y. Chen, X. Wang, W. Chen, S. Chen, and L. Hu, Materials (Basel). 15[21] (2022) 7439.
26. M.S. Bødker, R.E. Youngman, J.C. Mauro, and M.M. Smedskjaer, J. Phys. Chem. B. 124[45] (2020) 10292-10299.
27. J. Kjeldsen, M.M. Smedskjaer, J.C. Mauro, and Y. Yue, J. Non-Cryst. Solids. 406[15] (2014) 22-26.
28. K. Baral, A. Li, and W.Y. Ching, J. Phys. Chem. A. 121[40] (2017) 7697-7708.
29. A. Rodrigues, S. Fearn, and M. Vilarigues, J. Am. Ceram. Soc. 102[12] (2019) 7278-7287.
30. M.F. Dilmore, D.E. Clark, and L.L. Hench, J. Am. Ceram. Soc. 61[9-10] (1978) 439-443.
31. W. Zhifang, Z. Nai, M. Bo, and S. Zhongxin, J. Non-Cryst. Solids. 84[1-3] (1986) 468-476.
32. X. Wang, S. Fagerlund, J. Massera, B. Södergård, and L. Hupa, J. Mater. Sci. 52 (2017) 8986-8997.
33. Y. Onodera, Y. Takimoto, H. Hijiya, T. Taniguchi, S. Urata, S. Inaba, S. Fujita, I. Obayashi, Y. Hiraoka, and S. Kohara, NPG Asia Mater. 11 (2019) 75-85.
34. B. Ryu, in "Introduction to Glass Engineering" (Pusan National University Press, 2017) p. 78
35. J. Shen, D.J. Green, J. Non-Cryst. Solids. 344[1-2] (2004) 66-72.
36. H. Lammert and A. Heuer, Phys. Rev. B. 72[21] (2005) 214202.
37. W. Kingery, H.K. Bowen, and D.R. Uhlmann, in "Introduction to ceramics" (John wiley & sons, 1976) p. 152.
38. A. Fluegel, Eur. J. Glass Sci. Technol. 48[1] (2007) 13-30.
39. F. Iqbal, S. Kim, H. Yie, Y. Kim, and H. Kim, Ceram. Int. 42[8] (2016) 10393-10398.
40. A.A. El-Moneim, Mater. Chem. Phys. 52 (1998) 36-40.
41. K. Greene, M.J. Pomeroy, S. Hampshire, and R. Hill, J. Non-Cryst. Solids 325[1-3] (2003) 193-205.
42. J.E. Shelby, J. Am. Ceram. Soc. 66 (1983) 225-227.
43. Y. Onodera, S. Kohara, H. Masai, A. Koreeda, S. Okamura, and T. Ohkubo, Nat. Commun. 8 (2017) 15449.
44. K.V. Shah, M. Goswami, D.K. Aswal, V.K. Shrikhande, S.K. Gupta, and G.P. Kothiyal, J. Therm. Anal. Calorim. 89 (2007) 153157.
45. S. Sukenaga, T. Endo, T. Nishi, H. Yamada, K. Ohara, T. Wakihara, K. Inoue, S. Kawanishi, H. Ohta, and H. Shibata, Front. Mater. 8 (2021) 753746.
46. S.S. Sørensen, E.J. Pedersen, F.K. Paulsen, I.H. Adamsen, J.L. Laursen, S. Christensen, H. Johra, L.R. Jensen, and M.M. Smedskjaer, Appl. Phys. Lett. 117[3] (2020) 031901.
47. S.S. Sørensena, M.S. Bødker, H. Johra, R.E. Youngman, S.L. Logunov, M. Bockowski, S.J. Rzoska, J.C. Mauro, and M.M. Smedskjaer, J. Non-Cryst. Solids. 557 (2021) 120644.